



# The study of protostellar outflows with the SRT

C. Codella<sup>1</sup>, R. Bachiller<sup>2</sup>, J. Santiago<sup>2</sup>, and M. Tafalla<sup>2</sup>

<sup>1</sup> INAF - Istituto di Radioastronomia, Sez. di Firenze, Largo E. Fermi 5, I-50125 Firenze

<sup>2</sup> Observatorio Astronómico Nacional (IGN), Alfonso XII 3, E-28014, Madrid

**Abstract.** Protostars form in regions which are deeply hidden in molecular clouds and are surrounded by thick envelopes. Molecular outflows have the key to investigate the earliest evolutionary stages of star formation, especially at low luminosities where the outflow geometry can be relatively simple. In particular, the chemical changes induced by the passage of shocks associated with outflows can be used to try to establish an evolutionary scheme for outflows and consequently for the driving protostars. The main results obtained using mm-wavelength antennas during pilot projects focused on a small number of objects are shown. The strategy to carry on the project with the SRT is discussed.

## 1. Introduction and scientific background

Stars form in high-density regions of molecular clouds. As the circumstellar material is dispersed around a young stellar object (YSO) by the action of its outflow, the spectral energy distribution (SED) of the YSO evolves systematically. This process allowed the classification of YSOs in Classes 0, I, II, and III (e.g. André et al. 1993). However, this classification is too schematic, and thus under the label of Class 0 sources (e.g. sub-millimeter protostars) we find a rather heterogeneous collection of YSOs.

Outflows could have the key to refine the classification of YSOs, especially at low luminosities where flow geometry can be relatively simple. Mm-wave observations have put in evidence the properties of outflows: from Class 0 sources, which are highly collimated, to outflows from Class I sources, which are much less collimated and have a much lower mechanical power efficiency (Bontemps et al. 1996). The most recent observations show that there is also a kind of time sequence for low-

mass outflows based on well-known objects and on the chemical changes in the surrounding molecular outflows. The propagation of outflows and the consequent shock waves heat the surrounding medium and trigger chemical reactions, including also dust grains, that do not operate in more quiescent surroundings. The abundance of some species (such as SiO, CH<sub>3</sub>OH, H<sub>2</sub>O and several S-bearing molecules) can be therefore strongly enhanced (e.g. Bachiller 1996; Bachiller et al. 2001). Also a direct injection into the gas phase from the dust grain through sputtering can play a major role (e.g. Schilke et al. 1997; Caselli et al. 1997). Bachiller & Tafalla (1999) proposed a preliminary scheme based on a limited number of objects. The empirical time sequence can be summarised as follows (see also Santiago et al. 2005): (1) Jet-like outflows driven by Class 0 YSOs and associated with extremely high velocity (EHV) molecular bullets that appear as secondary components in the spectra, (2) Chemically active outflows which are driven by a Class 0, show no bullets, but are associated with very strong chemical anoma-

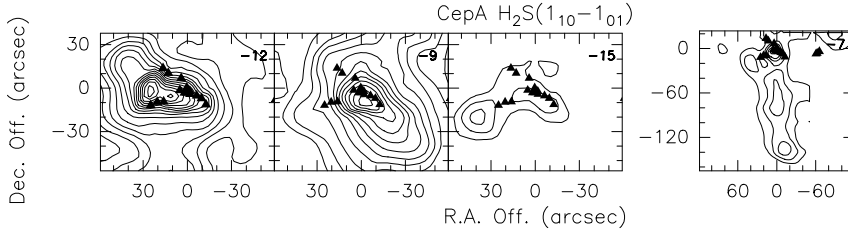


**Fig. 1.** Summary of the directions of the multiple outflows driven by the CepA-East YSOs as traced by the  $\text{H}_2\text{S}(1_{10}-1_{01})$  emission. Each panel shows the emission integrated over a velocity interval of  $1 \text{ km s}^{-1}$  centred at the value given in the upper right-hand corner (Codella et al. 2003). The triangles stand for the VLA 2-cm continuum components (Garay et al. 1996). At least four outflows are detected: the  $-12$  and  $-9 \text{ km s}^{-1}$  panels point out the NE and the SW directions, the  $-15 \text{ km s}^{-1}$  panel underlines a SE flow, while the  $-7 \text{ km s}^{-1}$  panel clearly indicates the occurrence of an outflow towards the south.

lies with large abundance enhancements and prominent wings in several shocked gas tracers, and (3) Class I outflows with no chemical anomalies and associated with evacuated cavities and HH objects. In other words, the chemically rich stage should be able to refine the low-mass protostar classification. In particular, the abundances of several molecules at the high velocities of the outflows can be used to further specify the characteristics of the Class 0 YSOs.

Unfortunately, the above classification is based on a few objects, and further unbiased observations are necessary to make it more detailed. The chemical anomalies have to be characterised in a sample of outflows from sources of similar low luminosity ( $\leq 10 L_{\odot}$ ), covering all of this empirical sequence. In addition, in order to check any possible dependence of the outflow's chemical richness on the star forming region (SFR) where the driving YSO is located, it would be fundamental to carry out a systematic study of the molecular outflows detected in nearby regions like Taurus, Perseus, Ophiuchus, or Serpens. The challenge is to find molecular species (i) whose production is exclusively associated with the high-temperature shocked gas, and (ii) whose abundance is clearly time-dependent to discern definitely the chemically active stage from the 1st and 3rd evolutionary phases. The answer can be found thanks to standard shock tracers such as SiO,  $\text{CH}_3\text{OH}$ , and  $\text{H}_2\text{O}$  as well as to products of the S-bearing chemistry such as SO,  $\text{HCS}^+$ , OCS,  $\text{H}_2\text{CS}$ , and  $\text{SO}_2$ . Actually, sul-

phur chemistry can be seriously affected by grain surface reactions: shock waves can inject  $\text{H}_2\text{S}$ , OCS, S into the gas phase with a consequent fast production of SO and  $\text{SO}_2$  (e.g. Pineau des Forêts et al. 1993; Charnley 1997; Wakelam et al. 2004). Once the gas phase has been enriched by the passage of a shock, other S-bearing species such as  $\text{H}_2\text{CS}$  and  $\text{HCS}^+$  are expected to significantly increase their abundances.

With this in mind, we decided to carry out with the 30-m IRAM antenna a deep millimeter survey of molecular lines towards a SFR with well-defined high-velocity components. Cepheus A well represents such a target: in particular the East component is associated with YSOs driving multiple outflows (e.g. Garay et al. 1996; Bergin et al. 1997, and references therein). Although CepA-East represents an intermediate-mass SFR with line emissions brighter than what is expected in  $L_{\text{bol}} \leq 10 L_{\odot}$  YSOs, it can be used as laboratory in which to study the variation of the abundances and excitation conditions along the line profiles. Actually, it is worth to stress the importance of studying in detail the line wings and the characteristics of the material flowing from YSOs as a function of the velocity: different excitation conditions as well as different gas compositions at different velocities are expected. In the light of results given by projects like that on CepA-East, it will be possible to plan routine studies of outflows driven by low-mass YSOs. The SRT antenna, given its capability to ob-

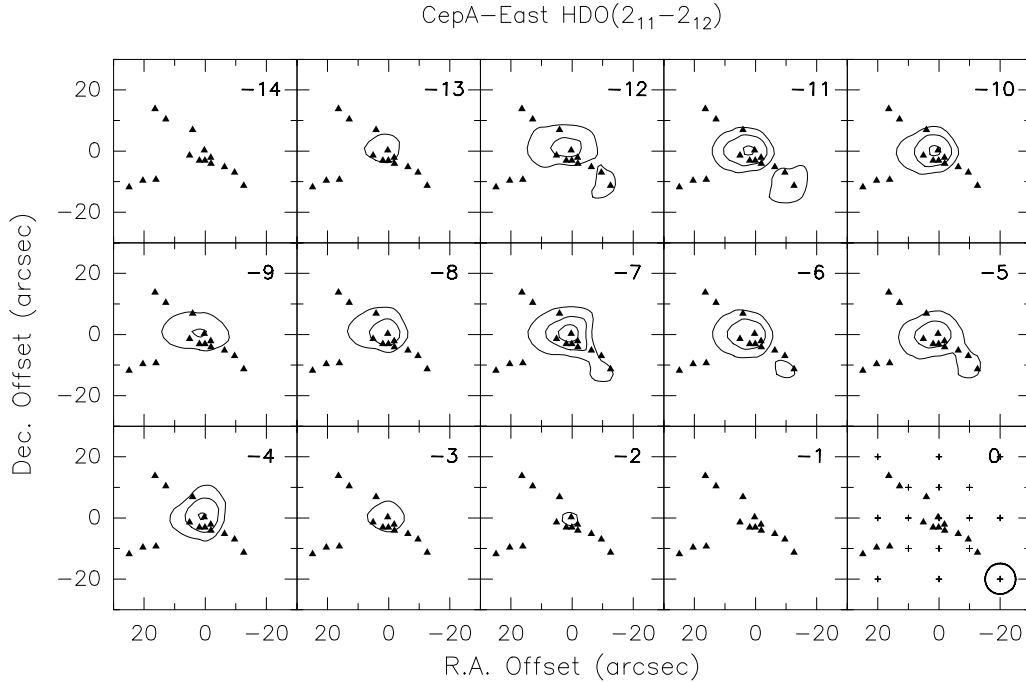


**Fig. 2.** Channel maps of the HDO( $2_{11}-2_{12}$ ) emission towards CepA-East (Codella et al. 2005). The empty circle shows the IRAM beam (HPBW), the small crosses mark the observed positions, while other symbols are drawn as in Fig. 1. The ambient velocity emission is  $-10.7 \text{ km s}^{-1}$ .

serve up to wavelengths close to  $\sim 3 \text{ mm}$ , will represent one of the best instruments to carry out the project. In Sect. 2 a brief summary of the main results obtained for CepA-East is presented, whereas in Sect. 3 a possible observing strategy with the SRT is proposed.

## 2. The pilot study of the CepA-East outflows

The results of the multi-line survey of CepA-East confirm the occurrence of several outflows. In particular, the  $\text{H}_2\text{S}$  observations allow us to improve the knowledge of this well-studied source. Trying to summarise the complex morphology, in Fig. 1 we report the most significant  $\text{H}_2\text{S}$  channel maps, comparing this emission with the ionised VLA jets observed by Garay et al. (1996). It is possible to detect the central outflow along the NE-SW direction (left panels), and the higher velocity eastern outflow from the central YSO cluster to

SE (middle panel): these motions had already been detected using CO emission (e.g. Bergin et al. 1997) and are well in agreement with the NE-SW VLA jets. In addition, the right panel of Fig. 1 shows the occurrence of high-velocity gas flowing from the YSOs' position towards the south. The present  $\text{H}_2\text{S}$  channel maps clearly show for the first time that CepA-East is associated with an intense and collimated southern outflow, confirming the importance of multiline molecular survey to unveil the SFR kinematics.

The HDO( $2_{11}-2_{12}$ ) channel maps (Fig. 2) report an additional evidence that the study of different molecules and different lines does not mean to simply reproduce the same gas distribution and that it can lead to tracing different gas associated with different physical and/or chemical conditions. This high-excitation ( $E_u = 95 \text{ K}$ ) HDO line shows: (i) a central component associated both with ambient velocity and high-redshift velocities, and (ii) a compo-

ment associated with the SW VLA chain. Since we cannot report here the spatial distributions relative to all the species observed, in Fig. 3 we report a schematic picture of the CepA-East as drawn by the multiline survey. It is worth noting that the southern outflow, not observed by the VLA, has been detected in  $\text{H}_2\text{S}$ ,  $\text{SO}_2$ ,  $\text{HDO}$ ,  $\text{H}_2\text{CS}$ , and  $\text{CH}_3\text{OH}$  and therefore it results chemically enriched with respect to the typical gas composition of the dark clouds. We refer the reader to Codella et al. (2003, 2005) for more details.

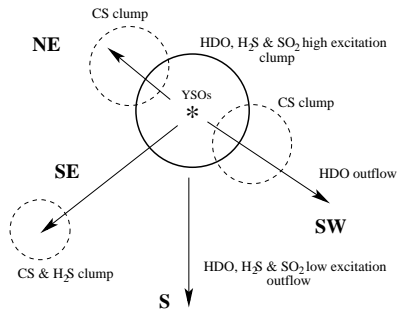


**Fig. 3.** A schematic picture (not to scale) of the directions of the multiple outflows driven by the CepA-East YSOs as traced by the multiline survey reported by Codella et al. (2003, 2005).

The most representative examples of line wings observed towards CepA-East are reported in Fig. 4. Different molecules exhibit different spectral behaviours: SiO and SO (as well as  $\text{H}_2\text{S}$  and  $\text{SO}_2$ , not shown here) are associated with extended profiles spanning the whole range of observed outflow velocities, whereas  $\text{HDO}$  and  $\text{H}_2\text{CS}$  (as well as  $\text{CH}_3\text{OH}$  and OCS) are associated with wings and, in addition, show a redshifted secondary peak at  $-5.5 \text{ km s}^{-1}$ , well-separated (by about  $5 \text{ km s}^{-1}$ ) from the ambient velocity. On the other hand, Fig. 5 reports the distribution with velocity of the brightness temperature ratio between  $\text{SO}(7-6)$  (upper panel),  $\text{SO}_2(5_{24}-4_{13})$  (middle panel),  $\text{H}_2\text{S}(1_{10}-1_{01})$  (lower panel) and  $\text{SiO}(5-4)$ . The comparison between the line profiles of different outflow tracers shows that SiO domi-

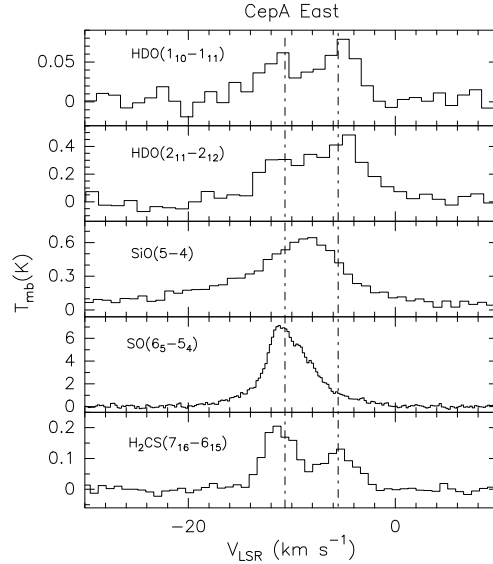


**Fig. 4.** Molecular line profiles observed towards CepA East: species and transitions are reported. The dashed lines stand for the ambient LSR velocity and for the component at  $-5.5 \text{ km s}^{-1}$  well-outlined e.g. in the  $\text{H}_2\text{CS}$  profile.

nates at the highest velocities, where the highest excitation conditions are found. This confirms the close association of SiO with shocks. On the other hand,  $\text{H}_2\text{S}$ ,  $\text{SO}_2$ , and SO preferentially trace more quiescent regions. In particular, we find a lack of a bright  $\text{H}_2\text{S}$  emission at the highest velocities. In addition,  $\text{H}_2\text{CS}$  and OCS emit at quite high velocities, where two shock tracers like  $\text{CH}_3\text{OH}$  and  $\text{HDO}$  increase their abundances. These results could indicate that  $\text{H}_2\text{S}$  is not the only major sulphur carrier in the grain mantles, and that OCS and  $\text{H}_2\text{CS}$  may probably play an important role on the grains; or that alternatively they could rapidly form once the mantle is evaporated after the passage of a shock.

### 3. SRT observing strategy

The final aim of the present project is to use the SRT in the effort to establish an evolutionary scheme for YSOs by investigating the chemical properties of the outflowing gas. The strategy is to observe a statistical sample of out-

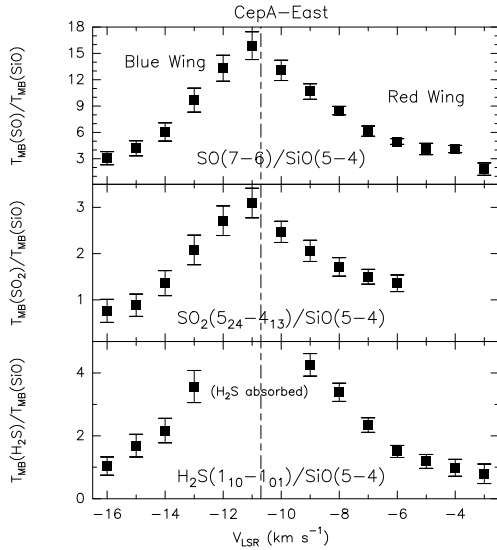


**Fig. 5.** Distribution with velocity of the ratio between the brightness temperatures of the SO(7–6) ( $E_u = 35$  K; upper panel), H<sub>2</sub>S(1<sub>10</sub>–1<sub>01</sub>) ( $E_u = 28$  K; middle panel), SO<sub>2</sub>(5<sub>24</sub>–4<sub>13</sub>) ( $E_u = 24$  K; lower panel) lines and of the SiO(5–4) ( $E_u = 21$  K) profile as detected towards CepA-East (Codella et al. 2005). The HPBW of the observations used here are: 9'' (SO), 10'' (SO<sub>2</sub>), and 11'' (H<sub>2</sub>S, SiO). The dot-dashed line marks the ambient LSR velocity.

flows in the lines of shock tracers as well as a tracer of the ambient medium, like C<sup>34</sup>S and N<sub>2</sub>H<sup>+</sup>, to well define the rest velocity. The selected molecules have almost all their emission lines at frequencies larger than 20 GHz. When possible, two or three lines of each species will be needed to discern between excitation and chemistry. Multi-receiver capabilities would make possible the simultaneous observations of the proposed lines, minimising the observing time, and avoiding problems of relative calibration and pointing. According to Brand et al. (2005), the SRT HPBW will be about 30''–48'' in the 20–50 GHz range and about 12'' at frequencies above 70 GHz. These values allow one to map different positions located along the outflow: for instance the size of the typical chemically rich outflow, L1157, is about 5', whereas the outflow associated with the typical Class 0 source, L1448, is ~4'.

The final list of the lines to observe will be selected in the next years and will be based on the results of forthcoming projects. In any case, examples of suitable lines can be found in the 20–50 GHz range, observable with the 4G, 5G, and 6G SRT receivers: C<sup>34</sup>S(1–0), SiO(1–0), CH<sub>3</sub>OH(1<sub>K</sub>–0<sub>K</sub>), HCS<sup>+</sup>(1–0), OCS(2–1), and H<sub>2</sub>CS(1<sub>01</sub>–0<sub>00</sub>). On the other hand, by using the 7G and 8G SRT receivers in the 70–110 GHz range it is possible to observe higher excitation lines: C<sup>34</sup>S(2–1), N<sub>2</sub>H<sup>+</sup>(1–0), SiO(2–1), CH<sub>3</sub>OH(2<sub>K</sub>–1<sub>K</sub>), HCS<sup>+</sup>(2–1), OCS(6–5), H<sub>2</sub>CS(3<sub>13</sub>–2<sub>12</sub>), SO(3<sub>2</sub>–2<sub>02</sub>), HDO(1<sub>10</sub>–1<sub>11</sub>), and SO<sub>2</sub>(3<sub>13</sub>–2<sub>02</sub>). In order to: (i) carefully investigate the line profile at high velocities, and (ii) detect EHV bullets, velocity resolutions of at least 0.2 km s<sup>–1</sup> and bandwidths larger than 100–200 km s<sup>–1</sup> are needed.

At this stage, only very preliminary time estimates can be done by using the values reported in Brand et al. (2005). By assuming a system temperature of ~70 K at 40 GHz, an rms of 0.02 (0.05) K should be reached in about 30 (5) minutes on-source. At 90 GHz, assuming a system temperature of 180 K one should have an rms of 0.03 (0.08) K again in 30 (5) minutes on-source. The derived rms values are low enough to detect the proposed lines with a good S/N ratio, since we expect brightness temperatures larger than 1 K for the CS, SO, and CH<sub>3</sub>OH lines, and about 0.1–0.5 K for the emission due to the other selected tracers (Codella & Bachiller 1999; Bachiller et al. 2001).

## References

- André, P., Ward-Thompson, D., & Barsony, M. 1993, *ApJ*, 406, 122  
 Bachiller, R. 1996, *ARA&A*, 34, 111  
 Bachiller, R., & Tafalla, M. 1999, in “The Origin of Stars and Planetary Systems”, (C.J. Lada, N.D. Kylafis, Eds.; Kluwer Academic Publishers, Dordrecht), p. 227  
 Bachiller, R., Pérez-Gutiérrez, M., Kumar, M.S.N., & Tafalla, M. 2001, *A&A*, 372, 899  
 Bergin, E.A., Ungerechts, H., Goldsmith, P.F., et al. 1997, *ApJ*, 482, 267

- Bontemps, S., André, P., Terebey, S., & Cabrit, S. 1996, *A&A*, 311, 858
- Brand, J., Caselli, P., Felli, M., Mack, K.-H., Poppi, S., Possenti, A., Prandoni, I., & Tarchi, A. (Eds.) 2005, “The Sardinia Radio Telescope (SRT). Science and technical requirements”, IRA Internal Report 371/05
- Caselli, P., Hartquist, T.W., & Havnes, O. 1997, *A&A*, 322, 296
- Charnley, S.B. 1997, *ApJ*, 481, 396
- Codella, C., Bachiller, R. 1999, *A&A*, 350, 659
- Codella, C., Bachiller, R., Benedettini, M., & Caselli, P. 2003, *MNRAS*, 341, 707
- Codella, C., Bachiller, R., Benedettini, et al. 2005, *MNRAS*, 361, 244
- Garay, G., Ramírez, S., Rodríguez, L.F., Curiel, S., & Torrelles, J.M. 1996, *ApJ*, 459, 193
- Pineau des Forêts, G., Roueff, E., Schilke, P., & Flower, D.R. 1993, *MNRAS*, 262, 915
- Santiago, J., et al. 2005, *in preparation*
- Schilke, P., Walmsley, C.M., Pineau des Forêts, G., & Flower, D.R. 1997, *A&A*, 321, 293
- Wakelam, V., Caselli, P., Ceccarelli, C., Herbst, E., & Castets, A. 2004, *A&A*, 422, 159